Journal of Materials Chemistry A

COMMUNICATION

Cite this: J. Mater. Chem. A, 2015, 3, 1925

Received 10th December 2014
Accepted 18th December 2014

DOI: 10.1039/c4ta06782g

www.rsc.org/MaterialsA

Continuous synthesis of size-tunable silver nanoparticles by a green electrolysis method and multi-electrode design for high yield†

Zhihai Huang,[a] Hao Jiang,[b] Peidang Liu,[c] Jianfei Sun,[a] Dawei Guo,[d] Jieling Shan[a] and Ning Gu*[a]

Although some methods have been developed, high-yield controllable synthesis of silver nanoparticles in aqueous solution is still challenging. Here, we report a green electrolytic synthesis of silver nanoparticles in a continuous flow system. Nanoparticle sizes could be tuned facilely by adjusting the flow velocity. Further, an improved multi-electrode electrolytic reactor was designed for increasing the yield.

Introduction

In the last decade, the synthesis of silver nanoparticles (AgNPs) in aqueous solution has received increasing attention due to their potential biomedical applications.[1–5] For biomedical applications, green synthesis and materials are desirable. However, liquid phase reduction is still the most common method and many harmful reagents are often used. Although AgNPs have already been controlled well in organic solutions,[6–9] the synthesis of AgNPs in aqueous solution is still challenging due to the hard-to-control nucleation process arising from the high reactivity of silver precursors in water.[10] Particularly, when amplifying the liquid phase reaction for large-scale synthesis of monodisperse AgNPs, the process is hard to control well because the synthesis conditions such as temperature and concentration might differ in micro-regions of a bigger reaction system owing to the limitation of heat and mass transfer.

Electrochemical synthesis is a facile, rapid and green method. It is mainly used to precipitate AgNPs on the surface of a substrate through the redox reaction taking place on/near the surface/interface of the electrode.[11–15] If the deposited AgNPs can be transferred efficiently from the surface of the substrate to the bulk solution, colloidal AgNPs can be obtained. Some groups synthesized AgNPs by the electrochemical reduction of silver salts,[16–18] though the syntheses need to be further controlled. Also, few reported that AgNPs could be directly synthesized by the electrolysis of pure silver, without adding any reducing agents and silver salts.[19,20] So the synthetic products may have higher purity than those synthesized by the general chemical reduction method, and are more suitable for biomedical applications. In addition, some assisted methods, for example, sonochemical technology, were also used to enhance the transfer of AgNPs from the substrate to the bulk solution.[21,22]

Recently, research has been conducted to synthesize large-scale AgNPs by electrochemical discharge in a continuous flow system, but the morphology and size are uncontrollable due to the violent discharge reaction conditions.[23] These studies motivated us to find ways to overcome such problems. Traditionally, electrochemical synthesis is seldom applied in a continuous flow system. We considered it meaningful to achieve control of electrochemical synthesis in a continuous flow system. This may combine the advantages of the electrochemical method and the continuous flow method. But there are some problems that need to be solved, for example, how to control the synthesis of AgNPs facilely and precisely, how to keep the reaction going on and prevent the passivation of the silver electrode, and how to increase the yield of AgNPs in unit time.

In this work, we developed a silver electrolytic reactor in a continuous flow system, and researched on the size control of AgNPs by facilely adjusting the flow velocity. To increase the synthesis yield of AgNPs in unit time, a hitherto unreported multi-electrode electrolytic reactor was designed.

Results and discussion

For the purpose of controllable synthesis of silver nanoparticles, we designed a silver electrolytic reactor in a continuous flow

[a]State Key Laboratory of Bioelectronics, Jiangsu Key Laboratory for Biomaterials and Devices, School of Biological Science and Medical Engineering, Southeast University, Nanjing, 210096, P.R. China. E-mail: guning.seu.edu.cn; Fax: +86-25-83272460; Tel: +86-25-83272476

[b]School of Electrical Engineering, Southeast University, Nanjing, 210096, P.R. China

[c]Institute of Neurobiology, School of Medicine, Southeast University, Nanjing, 210096, P.R. China

[d]College of Veterinary Medicine, Nanjing Agricultural University, Nanjing, 210095, P.R. China

† Electronic supplementary information (ESI) available: Photos and TEM images. See DOI: 10.1039/c4ta06782g

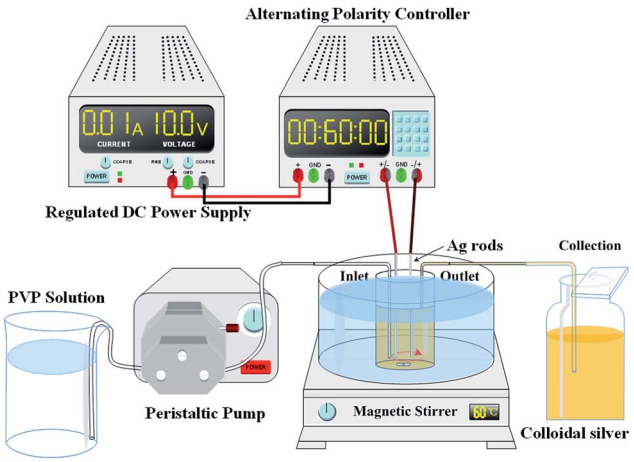

Scheme 1 Schematic of the electrolytic synthesis in a continuous flow system.

system as shown in Scheme 1. The reactor was an airtight cylinder container (Fig. S1†). Considering the homogenization of the reaction and the yield of AgNPs in unit time, the electrolytic cell was designed to a smaller volume (about 9.4 mL) with an inner diameter of 20 mm and height of 30 mm.

Two pure silver rods with a diameter of 2 mm and a length of 20 mm were fixed on the cover of the reactor as the anode and cathode, respectively. The center distance of the two electrodes was 8 mm. Regulated DC power supply was applied to the two electrodes through a homemade device called the "Alternating Polarity Controller". The input part, electrolytic reactor and output part are connected with two PTFE tubules, one extends close to the bottom of the reactor as the inlet for the reaction solution, and the other is embedded in the cover as the outlet for colloidal AgNP solution. The reaction solution is pumped into the reactor with a peristaltic pump and the synthetic products flow out of the outlet tube.

When synthesizing AgNPs in the reactor, the silver rod as the sacrificial anode will lose electrons and dissolve to form Ag^+. Near the anode oxygen gas is released due to the electrolysis of water; simultaneously, Ag_2O film is deposited on the surface of the anode. The migrated Ag^+ in the solution will be reduced to zero-valent Ag atoms on the cathode and hydrogen gas is released near the cathode. Under the attraction of van der Waals forces, Ag atoms nucleate and grow to AgNPs. The synthesized AgNPs are further transferred to the bulk solution from the cathode by vigorous stirring.

As shown in Fig. 1, formation of a thick oxidation deposition coating on the surface of the anode should be avoided. This is the key to a continuous electrolytic synthesis. The deposited Ag_2O film will lead to passivation of the silver electrode and hinder the electrolysis reaction. In addition, it easily dissolves many big impurity particles in the solution. Therefore, we designed an "Alternating Polarity Controller" to alternately change the polarities of the anode and cathode at intervals. The Ag_2O film may be reduced to Ag by released H_2 when the electrode is as a cathode. In this way, the oxide coating alternately deposited and dissolved on the surfaces of electrodes. So the

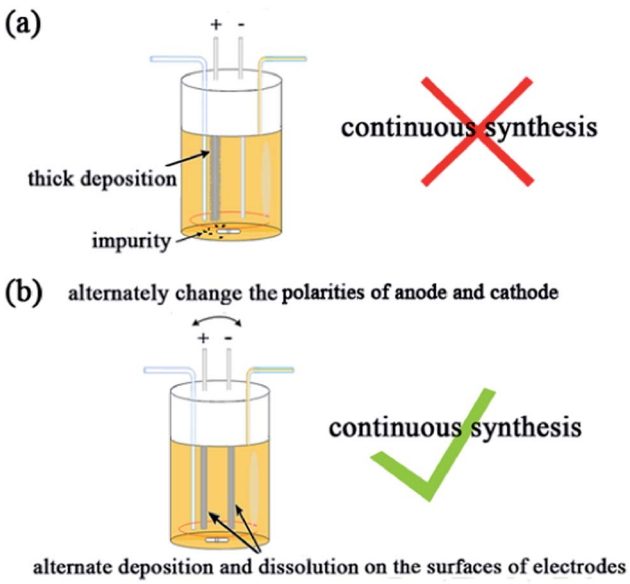

Fig. 1 The key factor for continuous electrolytic synthesis.

two silver electrodes can be consumed synchronously rather than sacrificing only one, and the continuous synthesis can be kept going. We can set the appropriate alternating time with the device, and the optimal alternating time will be determined in the future research.

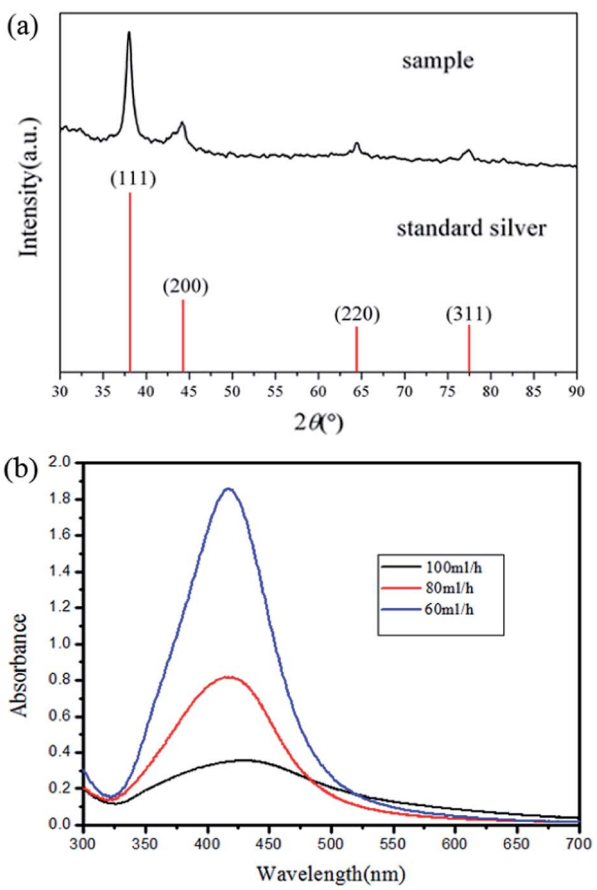

Fig. 2 (a) XRD pattern and (b) UV-Vis spectra of synthetic products.

The phase of the product can be determined by XRD. In Fig. 2(a), red lines show the standard XRD pattern of the simple substance "Ag" (JCPDS no. 04-0783).[24,25] It can be seen that the diffraction peaks of the product correspond to those of pure silver, and no peaks of impurities appear. Combining with XPS data analysis (Fig. S2†), we can confirm that the product is Ag rather than Ag_2O. The XRD pattern reveals that the product has good crystallinity and high purity. It is worth noting that the intensity rate of $I_{(111)}/I_{(200)}$ is higher than the standard value. It indicates that (111) planes tend to be preferentially oriented[9,26] (HRTEM in Fig. S3†). In Fig. 2(b), UV-Vis spectra of the products show that absorption peaks are all near 420 nm, which are assigned to the surface plasmon resonance of AgNPs.[24,27] We found the red shift of absorption peaks and the increase of absorbances with the decrease of flow velocity. It implies that the size and concentration of AgNPs increase when the flow velocity decreases, because the reaction solution may stay in the electrolytic cell for a longer time.

The size of AgNPs can be tuned facilely by adjusting the velocity of continuous flow solution. Fig. 3(a)–(c) show TEM images and size distributions of AgNPs synthesized with different flow velocities. As we expected, the flow velocity is faster; the synthesized AgNPs are smaller because of the shorter reaction and growth time. When the flow velocity is 60 mL h^{-1}, 80 mL h^{-1} and 100 mL h^{-1}, the average size (mean ± SD) of AgNPs is 18.5 ± 4.1 nm, 9.4 ± 1.5 nm and 3.0 ± 0.6 nm, respectively, and the AgNPs are all highly monodisperse. TEM results are consistent with previous UV-Vis spectra of AgNPs.

To enhance the yield of AgNPs in unit time, an improved multi-electrode electrolytic reactor was designed (Fig. S4†). The inner diameter and height of the electrolytic cell were increased to 40 mm and 50 mm, respectively. Eight silver rods with a diameter of 3 mm and a length of 40 mm were used as the anode and cathode, respectively. They were evenly arranged in the circle with a diameter of 20 mm at the cover of the reactor. Four non-adjacent silver rods were connected as a group of same polarity electrodes. The tubule at the bottom of the reactor was the inlet for reactive solution, and the other tubule at the cover center was the outlet for the product.

According to our measurement, the electrical conductivity of 5 mg mL^{-1} PVP aqueous solution is about 0.007 S m^{-1}. So, based on the solution's property and applied electrolytic voltage, the voltage distribution and electric field distribution in the multi-electrode electrolytic reactor were simulated and are shown in Fig. 4. We can see that the parallel anodes and parallel cathodes have the highest and lowest voltage distribution, respectively. According to the distribution simulation of the electric field, the facing surfaces of the two adjacent electrodes were the locations having the highest electric field intensity. The redox reactions of silver atoms and silver ions just happen there. In the electric field distribution diagram, the blue area that is close to the inside wall and the center of the reactor but away from the electrodes has no or weaker electric field intensity, and a relatively uniform ring electric field (the green area) forms along the arrangement of the eight electrodes. The ring electric field distribution is approximately consistent with the whirly flow movement of the solution under the agitating condition. Therefore, silver ions are suitable for transfer between the surface of adjacent electrodes along the ring arrangement of electrodes under the action of electric field and agitation. Although the volume of the electrolytic cell is increased several times, the number and length of silver electrodes are also increased in the synthesis system. This is equivalent to the simultaneous electrolysis of eight pairs of electrodes. In the reaction zone that is between the two adjacent

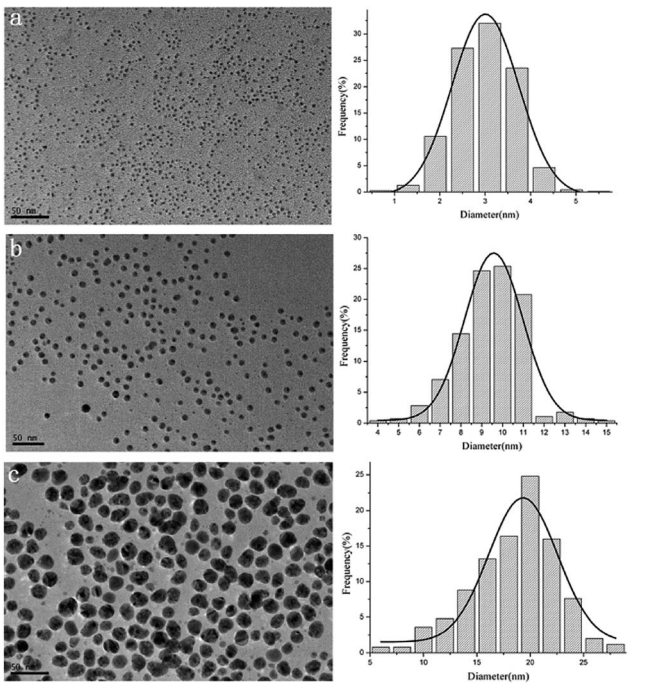

Fig. 3 TEM images and size distributions of AgNPs that were synthesized with different flow velocities: (a) 100 mL h^{-1}, (b) 80 mL h^{-1}, (c) 60 mL h^{-1}.

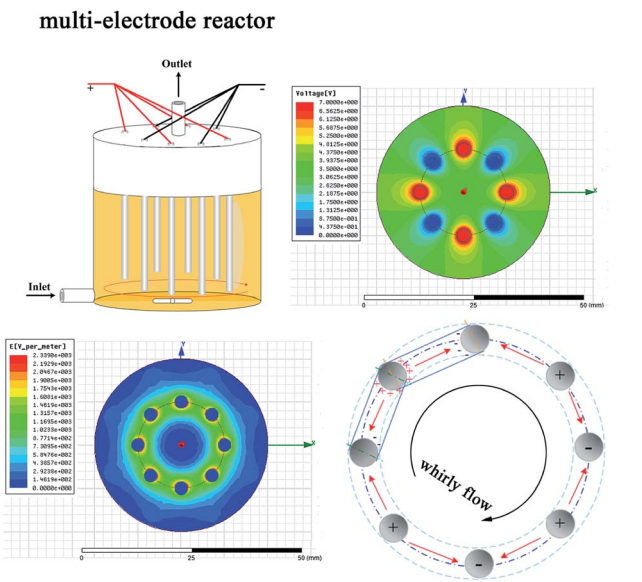

Fig. 4 Simulated diagrams of the voltage and electric field distribution in the multi-electrode electrolytic reactor.

electrodes, the synthesis is still in a smaller space and has a relatively uniform reaction conditions (the lower right part in Fig. 4). Therefore, the designed multi-electrode structure of the reactor can provide relatively uniform reactive conditions for the synthesis of the monodisperse and uniform AgNPs. In addition, we can prepare more Ag^+ and reduce them to AgNPs through electrolyzing multiple parallel electrodes simultaneously and thus the yield of AgNPs in unit time can be increased significantly. The synthesized colloidal solution may exhibit transparent brilliant yellow or brown yellow owing to the different sizes and concentrations (Fig. S5†). Similarly, the different sized highly monodisperse AgNPs can be synthesized by adjusting the flow velocity. For example, AgNPs with the size of 24.8 ± 4.7 nm, 11.4 ± 2.3 nm and 1.8 ± 0.6 nm are shown in Fig. S6.†

Conclusions

In summary, we proposed a green method that combined an electrochemical process and continuous synthesis strategy for the controllable synthesis of AgNPs in aqueous solution. We obtained a series of different sized AgNPs (about 1 nm to 30 nm) successfully by adjusting the velocity of the continuous flow. The AgNPs synthesized by this method have higher purity than those synthesized by common liquid phase reduction due to the absence of silver salts and harmful reducing agents during the synthesis. The monodispersity of AgNPs is also good because the reaction takes place in a smaller electrolytic cell instead of a bigger reaction volume all the time, and the output of AgNPs depends on the total continuous synthesis time. In addition, with an improved multi-electrode electrolytic synthesis system, the yield of AgNPs in unit time is significantly increased, whereas the morphology of AgNPs is still maintained.

Experimental

In the experiments, a good biocompatible polymer, polyvinyl pyrrolidone (PVP, K30), was used as the stabilizing agent, which was of analytical grade and used without further purification. Two silver rods with a diameter of 2 mm were used as electrolytic electrodes, and their purity was 99.9%. A classical synthesis process is as follows: firstly, the silver electrodes were polished, washed, and fitted on the cover of the electrolytic reactor. Secondly, 5 mg mL^{-1} PVP aqueous solution was prepared as the electrolyte and stabilizer. Finally, the PVP solution was pumped into the electrolytic reactor continuously by the peristaltic pump under a magnetic stirring condition at 60 °C, and a voltage of 10 V was applied to the silver electrodes simultaneously. The time for exchanging the polarities of the anode and cathode was set to 1 min through the "Alternating Polarity Controller". For synthesizing different sized colloidal silver nanoparticles, the flow velocity of 100 mL h^{-1}, 80 mL h^{-1} and 60 mL h^{-1} was used, respectively. The process of the multi-electrode electrolytic synthesis is similar to this, and the details are given in the ESI.† The phase composition of the product was analyzed with an X'TRA Powder X-ray Diffraction Instrument (ARL, Switzerland) with CuKα radiation. The spectrum of the product was examined from 800 nm to 300 nm by a UV-3600 UV-Vis spectrophotometer (Shimadzu, Japan). The morphology of the synthesized nanoparticles was characterized by a JEM-2000EX Transmission Electron Microscope (JEOL, Japan) and the size distribution was determined by counting all nanoparticles in TEM photographs. The chemical state of silver nanoparticles was investigated using X-ray photoelectron spectroscopy (XPS, PHI 5000 VersaProbe, UIVAC) with an Al Kα radiation as the X-ray source.

Acknowledgements

This work was supported by the National Key Basic Research Program of China (2013CB933904, 2011CB933503, 2013CB733801), the National Natural Science Foundation of China (51201034, 20903021, 21273002), the Natural Science Foundation of Jiangsu Province (BK2011036, BK2011590, BK20140716), the International Postdoctoral Exchange Fellowship Program, the Research Fund for the Doctoral Program of Higher Education of China (20090092120036) and the special fund for the top doctoral thesis of Chinese Education Ministry.

Notes and references

1 Z. H. Huang, X. L. Jiang, D. W. Guo and N. Gu, *J. Nanosci. Nanotechnol.*, 2011, **11**, 9395.
2 M. Ahamed, M. S. AlSalhi and M. Siddiqui, *Clin. Chim. Acta*, 2010, **411**, 1841.
3 X. Chen and H. J. Schluesener, *Toxicol. Lett.*, 2008, **176**, 1.
4 A. Ravindran, P. Chandran and S. S. Khan, *Colloids Surf., B*, 2013, **105**, 342.
5 S. Eckhardt, P. S. Brunetto, J. Gagnon, M. Priebe, B. Giese and K. M. Fromm, *Chem. Rev.*, 2013, **113**, 4708.
6 Y. Sun, *Chem. Soc. Rev.*, 2013, **42**, 2497.
7 L. Li, J. Sun, X. R. Li, Y. Zhang, Z. X. Wang, C. R. Wang, J. W. Dai and Q. B. Wang, *Biomaterials*, 2012, **33**, 1714.
8 C. Chen, L. Wang, H. J. Yu, J. J. Wang, J. F. Zhou, Q. H. Tan and L. B. Deng, *Nanotechnology*, 2007, **18**, 115612.
9 Y. Gao, P. Jiang, L. Song, J. X. Wang, L. F. Liu, D. F. Liu, Y. J. Xiang, Z. X. Zhang, X. W. Zhao, X. Y. Dou, S. D. Luo, W. Y. Zhou and S. S. Xie, *J. Cryst. Growth*, 2006, **289**, 376.
10 Y. Wan, Z. Guo, X. Jiang, K. Fang, X. Lu, Y. Zhang and N. Gu, *J. Colloid Interface Sci.*, 2013, **394**, 263.
11 S. C. Tang, X. K. Meng, C. C. Wang and Z. H. Cao, *Mater. Chem. Phys.*, 2009, **114**, 842.
12 B. J. Yang, N. Lu, C. Y. Huang, D. P. Qi, G. Shi, H. B. Xu, X. D. Chen, B. Dong, W. Song, B. Zhao and L. F. Chi, *Langmuir*, 2009, **25**, 55.
13 G. M. Chapman, H. Bai, C. Li and G. Q. Shi, *Mater. Chem. Phys.*, 2009, **114**, 120.
14 X. Y. Zhang, J. Zhao and R. P. Van Duyne, *Nano Lett.*, 2005, **5**, 1503.
15 Y. H. Zhang, J. H. Zhuang, D. J. Wang and A. G. Dong, *Chem. Commun.*, 2002, 2814.
16 B. S. Yin, H. Y. Ma, S. Y. Wang and S. H. Chen, *J. Phys. Chem. B*, 2003, **107**, 8898.

17 H. Y. Ma, B. S. Yin, S. Y. Wang, Y. L. Jiao, W. Pan, S. X. Huang, S. H. Chen and F. J. Meng, *ChemPhysChem*, 2004, **5**, 68.
18 P. Y. Lim, R. S. Liu, P. L. She, C. F. Hung and H. C. Shih, *Chem. Phys. Lett.*, 2006, **420**, 304.
19 M. Z. Hu and C. E. Easterly, *Mater. Sci. Eng., C*, 2009, **29**, 726.
20 R. A. Khaydarov, R. R. Khaydarov, O. Gapurova, Y. Estrin and T. Scheper, *J. Nanopart. Res.*, 2009, **11**, 1193.
21 S. C. Tang, X. K. Meng, H. B. Lu and S. P. Zhu, *Mater. Chem. Phys.*, 2009, **116**, 464.
22 Y. C. Liu and L. H. Lin, *Electrochem. Commun.*, 2004, **6**, 1163.
23 K. Tseng, Y. Chen and J. Shyue, *J. Nanopart. Res.*, 2011, **13**, 1865.
24 B. Chen, X. L. Jiao and D. R. Chen, *Cryst. Growth Des.*, 2010, **10**, 3378.
25 Y. X. Hu, J. P. Ge, D. Lim, T. R. Zhang and Y. D. Yin, *J. Solid State Chem.*, 2008, **181**, 1524.
26 Y. G. Sun and Y. N. Xia, *Science*, 2002, **298**, 2176.
27 G. A. Martinez-Castanon, N. Nino-Martinez and F. Martinez-Gutierrez, *J. Nanopart. Res.*, 2008, **10**, 1343.